▌**Crystal Engineering** |*Hot Paper*|

# Crystal Engineering with Multipoint Halogen Bonding: Double Two-Point Donors and Acceptors at Work

David Bulfield,* Elric Engelage, Lucas Mancheski, Julian Stoesser, and Stefan M. Huber*[a]

**Abstract:** The combination of singly or doubly bidentate halogen-bond donors with double bidentate acceptors was investigated as a supramolecular synthon in crystal engineering. The crystal topologies obtained feature novel halogen-bonding motifs like double two-point recognition and infinite chains or networks based on two-point interactions. Induced conformational changes in the double bidentate halogen-bond donors could be exploited to obtain different 1D and 2D networks. All solid-state studies were accompanied by DFT calculations to predict and rationalize the outcome.

## Introduction

Halogen-bonding (XB) is a noncovalent interaction between an electrophilic halogen substituent and a Lewis base.[1] Even though the interaction is closely related to hydrogen bonding (HB), it had received little attention until the 1990s.[2] Spearheaded by the work of Metrangolo and Resnati,[3] halogen bonding was then introduced as a reliable tool for crystal engineering.[3a, 4] Subsequently, predominantly applications in the solid state followed these first examples.[5] Nevertheless, in recent years an increasing number of applications in the liquid phase have also been reported, for example, in anion recognition,[6] anion transport,[7] catalysis, and related fields.[8]

These investigations and many theoretical studies[9] revealed some of the unique features that distinguish halogen bonding from hydrogen bonding.[10] Among others, one of these features is the high linearity of the interaction, resulting in a ≈180° angle for R—X•••B (R—X = halogen-based Lewis acid/ XB donor, B = Lewis base). This property can be utilized to design and predict patterns in the solid state, ranging from 1D and 2D infinite chains to more sophisticated 3D networks.[5a, 11] However, the overwhelming majority of these studies are based on single-point interactions, mostly with spherical anions like halides as multidentate Lewis bases.[5d, 12] In con-

trast, studies involving multipoint halogen-bonding interactions are rare. In fact, the design of such systems is more challenging for XB compared to HB due to said directionality, which demands very well-fitting donor/acceptor pairs.

A two-point binding motif was realized by Berryman et al. in the coordination of perrhenate by a cationic bidentate XB donor.[6e] In terms of neutral substrates, our group recently showed that oxadiazoles can be bound twofold by polyfluorinated and -iodinated terphenyls acting as neutral bidentate XB donors.[13]

In addition, Ouahab et al. reported a two-point S•••I interaction between an iodinated tetrathiofulvalene derivative and a thioisocyanato metal complex.[14] Other studies employed molecules containing both donor and acceptor functionalities with complementary binding sites to form dimers.[15] Beyond these two-point interactions, only a few examples of multipoint binding were reported. Our group described a three-point interaction between an orthoamide and a tridentate halogen-bond donor.[16] Even more complex structures have been designed by the groups of Aakeroy[17] and Diederich[18] in the form of halogen-bond-based molecular capsules. In parallel, Taylor and co-workers have published work on halogen bonding polymers that contain multiple XB donor or acceptor moieties on individual polymer chains.[19] Thus, to the best of our knowledge, multipoint interactions have so far almost exclusively[20] been employed in isolated 1:1 complexes (like molecular capsules). Herein, we aim to advance from these cases towards larger supramolecular assemblies (like infinite chains and networks). An overview of the topologies considered in this publication is given in Figure 1. The ultimate goal is to introduce such multipoint XB donor/acceptor motifs as synthons in crystal engineering.

Obviously, such studies crucially rely on the use of at least double bidentate halogen-bond donors and acceptors. This brings with it the question of cooperativity, that is, how conformational changes induced by the first binding event influence the behavior of the second binding site. We demonstrate

[a] *Dr. D. Bulfield, E. Engelage, L. Mancheski, J. Stoesser, Prof. Dr. S. M. Huber*
*Faculty of Chemistry and Biochemistry*
*Ruhr-Universität-Bochum*
*Universitätsstraße 150, 44801 Bochum (Germany)*
*E-mail: david.bulfield@rub.de*
*         stefan.m.huber@rub.de*

□ *Supporting information and the ORCID identification number(s) for the author(s) of this article can be found under:*
*https://doi.org/10.1002/chem.201904322.*

**This Work:**



double bidentate XB-donor

bidentate XB-donor

double bidentate XB-acceptor

double bidentate XB-acceptor (binding twice)

double two-point recognition

infinite two-point chain

2D-networks based on tetradentate XB-donors an acceptors

infinite chains with alternating binding modes due to conformational change

infinite chains with alternating binding modes and two different XB-acceptors

**Figure 1.** Schematic representation of the different halogen-bonding motifs which were obtained in the solid state in this study.

Halogen bond donors        Halogen bond acceptors
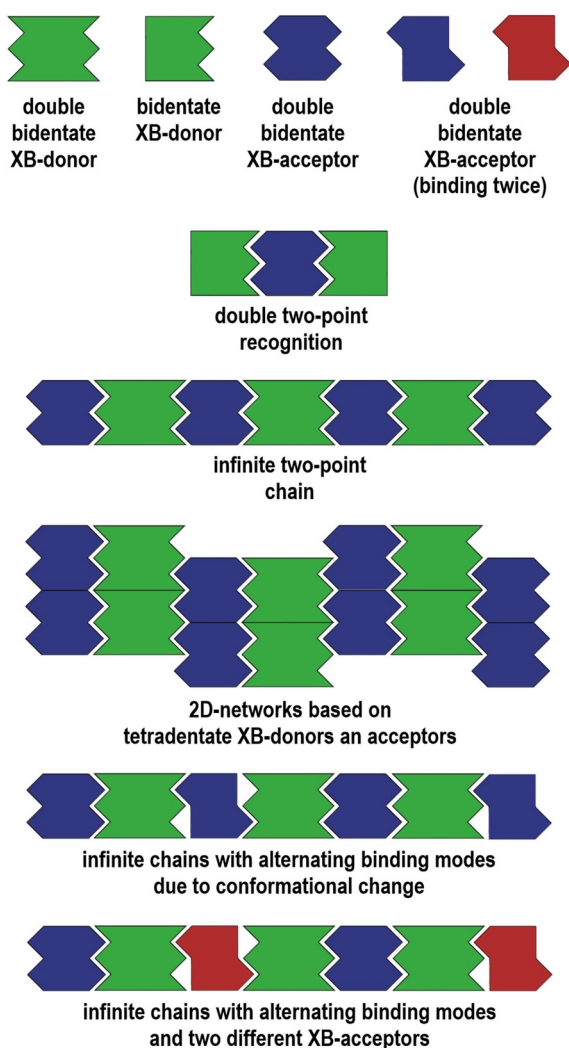


*p*4I, *syn-p*2I

*m*4I, *syn-m*2I

1

2

**Figure 2.** Schematic representation of the different halogen-bonding motifs which were obtained in the solid state in this study.

how this effect can be predicted and analyzed by DFT calculations and how it can be used as a tool to obtain different 1D and 2D networks.

## Results and Discussion

As mentioned above, two-point-bound 1:1 complexes had already been obtained in the solid state between tetraiodinated XB donor **m4I** (Figure 2) and an oxadiazole, in which the two nitrogen atoms served as the XB acceptor moieties.[13] Hence, this XB donor as well as its diiodinated analogue (*syn-***m2I**) and their *para*-substituted counterparts (**p4I** and *syn-***p2I**) were chosen as lead structures. However, the two-point interaction with oxadiazoles had been proven to be very weak by DFT calculations and NMR titrations in solution, with a binding constant to XB donor *syn-***m2I** of only $K \approx 2 \, M^{-1}$ in toluene. Therefore, stronger halogen-bond acceptors had to be found and as a consequence nitrogen-containing aromatic heterocycles were not further considered for this study, since their Lewis ba-
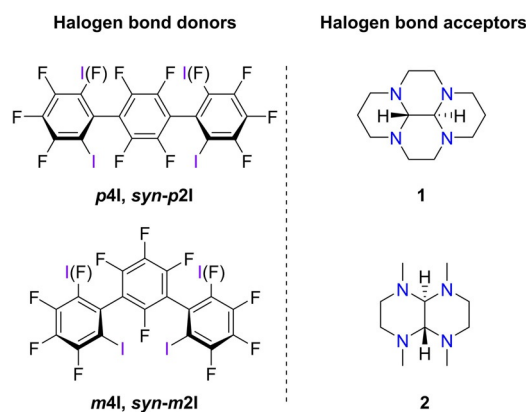
sicity is usually much lower compared to their saturated counterparts. In addition, oxadiazoles are also only singly bidentate XB acceptors, and there is no straightforward option to synthesize double bidentate versions.

In the search for suitable XB acceptors with four Lewis basic atoms, candidate structures were inspired by our previously reported three-point recognition study, in which an orthoamide was used.[16] This had resulted in a binding constant in the order of $10^4 \, M^{-1}$ in cyclohexane. Furthermore, orientating titration experiments indicated that this motif can also be transferred to two-point recognition, as reasonably strong binding was detected between *N,N*-dimethyl hexahydropyrimidine and *syn-***m2I** ($K \approx 42 \, M^{-1}$) or *syn-***p2I** ($K \approx 17 \, M^{-1}$) in solution (cyclohexane).

Based on these initial thoughts and with the help of DFT calculations, *trans*-decahydrotetraazapyrene **1** (Figure 2) was identified as a suitable multidentate Lewis base. Its highly rigid structure is similarly preorganized as the orthoamide mentioned above. Importantly, the rigidity of the structure also suppresses nitrogen inversions, which in general leads to a higher Lewis basicity of the nitrogen atoms.[21]

At first, "one-sided" XB donor *syn-***p2I**[13] (with two iodine substituents on one side of the molecule) was co-crystallized with substrate **1** in an effort to obtain a 2:1 complex, which could serve as a model system for extended networks. The obtained co-crystal (Figure 3) indeed featured the desired double two-point recognition motif in which every nitrogen atom is bound to one iodine atom through halogen bonding. It is immediately obvious, however, that the terphenyl backbones of the XB donors are bent (Figure 3, top). While we had already observed this in the past in the binding of iodinated terphenyls with halides,[8c] it can be assumed that this has a cost in terms of binding energy. The lengths of the halogen bonds are in the range of a typical N—I halogen bond (3.06 and 3.02 Å). In some contrast to this, the C—I···N bond angles (165°) deviate a bit from the usual ≈180°. An inspection of the binding motif from an orthogonal point of view (Figure 3, bottom) illustrates the Z-like pattern and also shows the parallel alignment of the terphenyls. The central benzene ring is not only bent (as described above) but also tilted away from a perfectly perpendic-
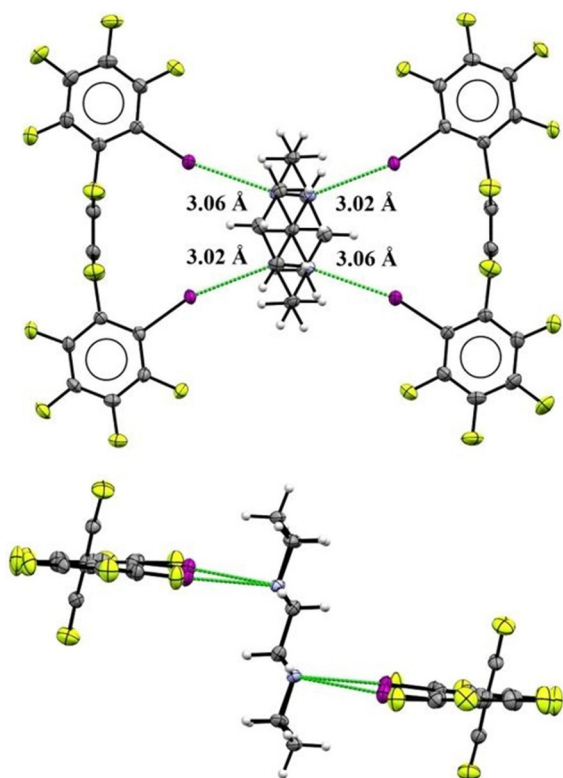
**Figure 3.** Co-crystal structure obtained by XRD between XB acceptor **1** and *syn*-**p2I** forming a two-point recognition based 2:1 complex (ellipsoids at 50% probability). Halogen bonds are highlighted in green including their corresponding binding distance.

ular orientation with respect to the outer phenyl rings. This is a re-occurring motif in other crystal structures described below and a geometrical feature which can also be found in all corresponding DFT calculations.

For comparison, we also crystalized linker **1** with the corresponding *anti*-conformer ***anti*-p2I** (Figure 4). This compound is of course not expected to form a similar 2:1 complex like the *syn* variant. Instead, an infinite chain was found in which XB acceptor **1** is bound once on each side. In this case the central aromatic ring of the terphenyl backbone is not bent. Since there is no bidentate coordination, there is also less constraint onto the formation of the halogen bond. This results in two
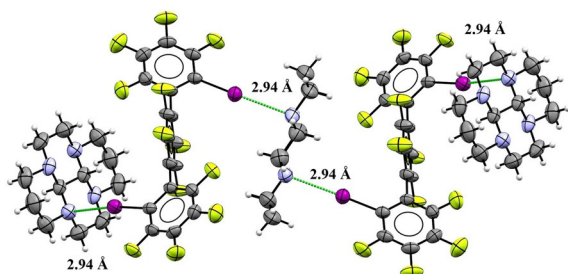


**Figure 4.** Cocrystal structure obtained by XRD between XB acceptor **1** and ***anti*-p2I** forming an infinite chain based on single-point interactions (ellipsoids at 50% probability). Halogen bonds are highlighted in green including their corresponding binding distance.

shorter (both 2.94 Å) and more linear halogen bonds (∢171° and ∢172°).

In crystal engineering studies based on single-point halogen bonding, the formation of infinite chains is often observed.[5e] Hence, the next goal was to investigate whether similar structures could also be obtained based on two-point recognition, using the motif shown in Figure 3 top. To this end, we used the two-sided (tetraiodinated) halogen donor **p4I**, which we had employed as organocatalyst previously.[8c]

However, the cocrystallization of said **p4I** with linker **1** did not yield the desired outcome: instead of a twofold two-point binding, only one side of **p4I** was bound in the latter fashion, while on the other side two moieties of Lewis base **1** were coordinated (Figure 5). While one of these halogen bonds was relatively short and linear (2.97 Å, ∢170°), the other ones were markedly longer and deviated more from the ideal 180° (for instance: 3.48 Å, ∢154°). Likewise, the halogen-bond acceptor (**1**) was also two-point-bound on one side and double single-point-bound on the other side. The reason why this topology is formed instead of an infinite chain is the bending of the central part of the terphenyl backbone. On the one hand, this de-
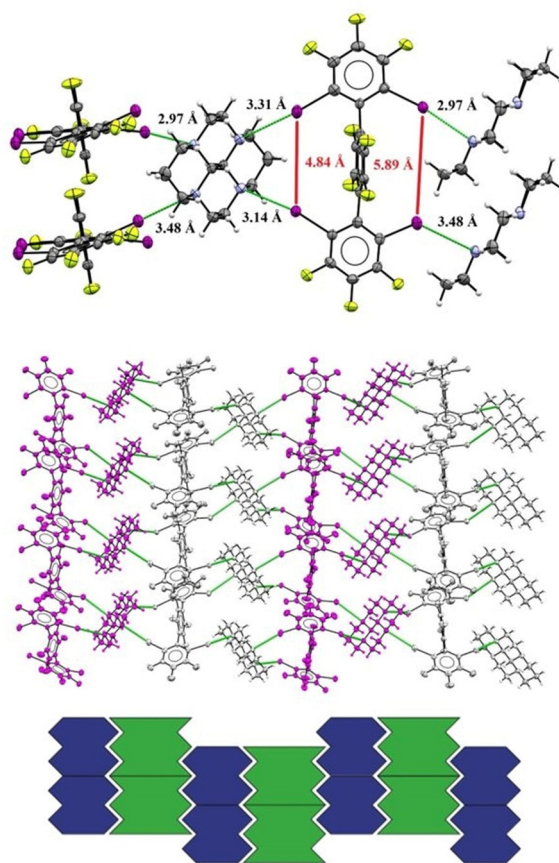


**Figure 5.** Top: Co-crystal structures of halogen-bond donor **p4I** with linker **1**, as obtained by XRD (ellipsoids at 50% probability). Halogen bonds are highlighted in green with their corresponding binding distance. Middle: 2D network formed by double bidentate halogen-bond donors and acceptors. The halogen-bonded left-handed helix is highlighted in magenta. The corresponding right-handed helix is shown in white. Bottom: Schematic representation of the crystal structure topology with the tetradentate halogen-bond donors (green) and acceptors (blue).

formation is necessary to allow two-point recognition similarly to the co-crystal of *syn-p2I* and **1**. On the other hand, this also increases the distance between the iodine substituents on the opposite side (4.84 vs. 5.89 Å, see Figure 5) which makes it impossible to form a second two-point interaction with **1** on this second side. Nevertheless, every nitrogen and iodine atom is bound to a counterpart and, therefore, a 2D network is formed (Figure 5 bottom). Overall, two helical structures with opposite handedness are formed by the single-point interactions (colored magenta and white in Figure 5), which are then connected to each other by the two-point contacts.

As we did not obtain the desired infinite-chain-type structure, we searched for a double bidentate amine in which the two amines on each binding site are further away from each other than in linker **1**. For this purpose, we synthesized compound **2** according to Willer and co-workers.[22] This compound has four methyl groups instead of the two propyl linkers. Due to the steric hinderance of the methyl groups towards each other, the whole molecule is twisted and less planar. As a consequence, the two nitrogen lone pairs which point to the same side of the molecule are now in a 1,4-distance (compared to the 1,3-distance in linker **1**) and are therefore further away from each other (see Figure 6). Another difference concerns
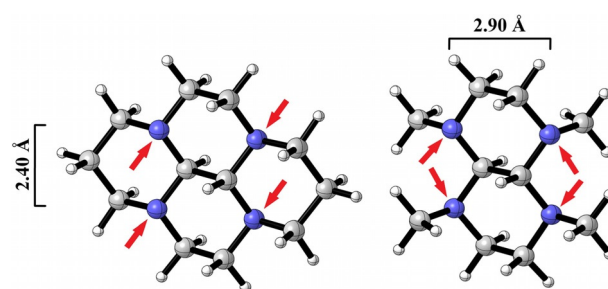


**Figure 6.** Double bidentate halogen acceptors **1** (left) and **2** (right) used within this study as obtained by DFT-calculations (M06-2X/def2-TZVP). The directions of the binding interactions are indicated by the red arrows.

the bite angle of the molecule, as the two amine electron-pairs are not parallel to each other like in compound **1**. This should provide a better fit to the halogen-bond donor atoms in *p4I*, which are also not orientated perfectly parallel to each other.

Compound **2** could be co-crystallized with all three previously mentioned halogen bond donors. The co-crystal of *syn-p2I* with **2** featured a double two-point motif (similar to the adduct of *syn-p2I* with linker **1**; see Figure 7A). As expected, for each two-point coordination, the corresponding nitrogen
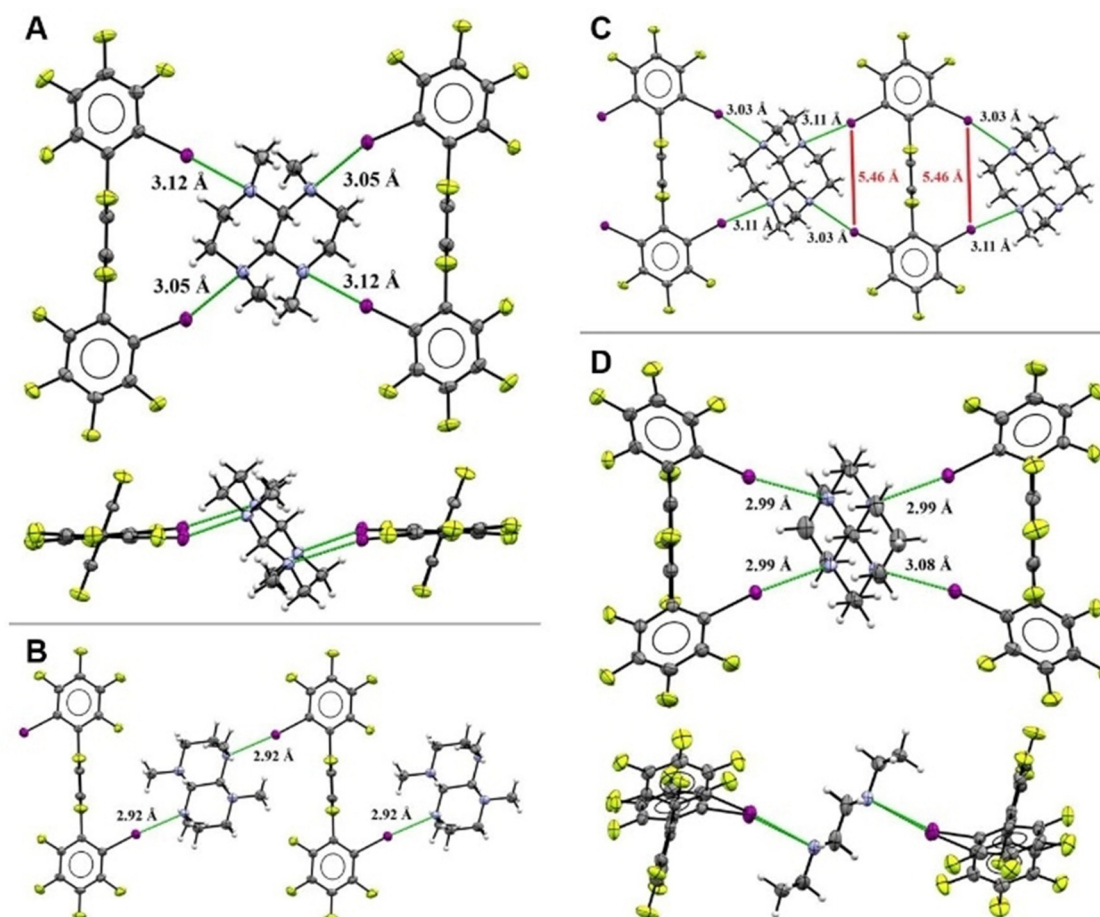


**Figure 7.** Co-crystal structures as obtained by XRD analysis. All ellipsoids at 50% probability and halogen bonds are highlighted in green with their corresponding binding distance. **A**: Co-crystal of **2** and *syn-p2I* forming a 2:1 complex based on two-point recognition. **B**: Co-crystal of **2** and *anti-p2I* which form a 2D-infinite chain based on single point interactions. **C**: Co-crystal of **2** and *p4I* which form an infinite chain based on two-point recognition. Distances between the iodine atoms are highlighted in red. **D**: Co-crystal structure of **1** and *syn-m2I* which form a 2:1 complex based on two-point recognition.

substituents were in a 1,4-distance, which resulted in a nearly unperturbed terphenyl backbone of the halogen-bond donor. A view along the terphenyl axis (Figure 7 A bottom) reveals that the halogen bonds are not as linear as in the previous case with linker **1**. Also, the binding distances are slightly larger (3.12 and 3.05 Å).

In addition, we also obtained the co-crystal between ***anti-p*2I** and halogen-bond acceptor **2**, which had a similar zig-zag-chain-like topology as the corresponding co-crystal with compound **1** (Figure 7 B).

Since the bending distortion of the terphenyl backbone of ***syn-p*2I** was much less pronounced with linker **2** compared to linker **1**, we were now able to obtain the aspired two-point-based infinite-chain motif in the co-crystal of the former with **p4I** as halogen-bond donor (Figure 7 C). The binding distances (3.11/3.03 Å) and angles were very similar to the 2:1 complex of ***syn-p*2I** with **2**. The iodine–iodine distance on each side of the molecule (5.46 Å) was in-between the asymmetric ones measured in the cocrystal of **p4I** and **1**.

Now that a suitable acceptor had been found for **p4I** to allow the formation of a two-point infinite chain, we wondered whether the same crystal topology could be obtained with linker **1** by employing a more suitable halogen-bonding counterpart. Therefore, we co-crystallized tetramine **1** with the *meta* derivatives ***syn-m*2I** and **m4I**. In these molecules, the iodine atoms are closer to each other due to the 1,3-terphenyl backbone. In addition, the halogen-bond donors can adapt better to the geometry of the acceptor via rotation around the C—C

bonds between the aromatic rings. This can either bring the iodine substituents closer together or further away from each other.

The co-crystal of ***syn-m*2I** and **1** (Figure 7 D) features, at first glance, the same double two-point motif which was already found for *syn*-p2I (Figure 2). However, the core structure of the halogen-bond donor shows almost no bending deformation at all. Rather, a view perpendicular to the plane of the tetramine (Figure 7 D, bottom) clearly indicates that there is some rotation around the C—C single bonds connecting the phenyl moieties (which alters the intramolecular iodine–iodine distances).

This is also the case for the co-crystal of ***anti-m*2I** with linker **1**, in which the terphenyls are also not orthogonal to each other (Figure 8 A). In essence, the structure of this co-crystal features the same zig–zag single-point motif that had been found in the adduct of the *para*-isomer ***anti-p*2I** with both tetramines.

The variability of the iodine–iodine distance in **m4I** (enabled by the C—C bond rotations) had implications for its co-crystal with linker **1**. In a first crystallization attempt, the aspired two-point recognition infinite chain was not obtained (Figure 8 B). Instead, only one side of **m4I** was two-point coordinated by the tetramine, while the other side was only bound once, similarly to the co-crystal of **p4I** and linker **2**. Here, however, a different type of network topology was formed, as two iodine atoms of different halogen-bond donors bind to each other via a type I halogen–halogen contact.[5f, 23] This, in combination with the double two-point recognition motif, results in a 1D-in-
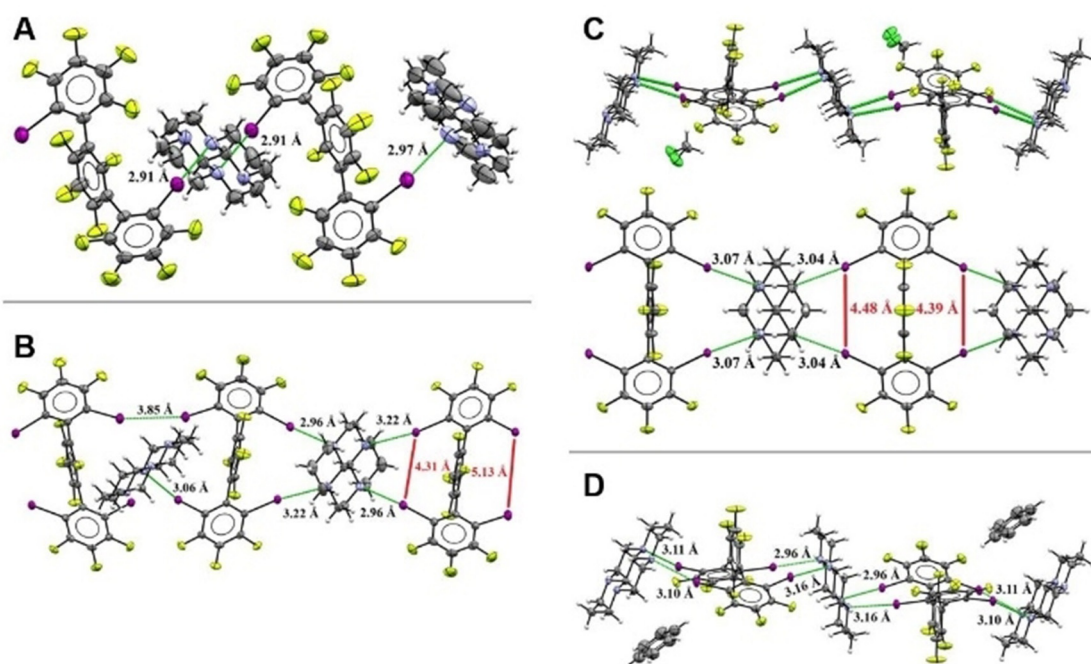


**Figure 8.** Co-crystal structures as obtained by XRD analysis. All ellipsoids at 50% probability and halogen bonds are highlighted in green with their corresponding binding distance. Distances between the iodine atoms are highlighted in red. A: Co-crystal of tetramine **1** and halogen bond donor ***anti-m*2I**, which forms a 2D infinite chain. B: Co-crystal of linker **1** and terphenyl **m4I** *obtained from pentane* forming an infinite chain with alternating binding modes: one acceptor is bound by a double bidentate interaction, while the other is bound via single-point interactions. Additionally, a type I halogen–halogen contact connects two iodine atoms. C: Co-crystal of **1** and **m4I** obtained from dichloromethane which forms an infinite chain based on two-point recognition. The dichloromethane molecules have short contacts to both the donor and acceptor molecules (not shown). In the bottom view dichloromethane molecules are omitted for clarity. D: Co-crystal of **1** and **m4I** obtained from benzene which also forms an infinite chain based on two-point recognition.

| Table 1. Computed binding enthalpies and Gibbs free energies for the first and second binding events of the halogen bond donors with 1 and 2.[a] | | | | | | | | |
|---|---|---|---|---|---|---|---|---|
| Donor [D] | *syn-p*2I | | *p*4I | | *syn-m*2I | | *m*4I | |
| Acceptor [A] | 1 | 2 | 1 | 2 | 1 | 2 | 1 | 2 |
| First binding [D—A] | | | | | | | | |
| $\Delta H$ [kcal mol$^{-1}$] | −15.4 | −15.4 | −15.6 | −14.9 | −16.7 | −15.3 | −16.9 | −14.4 |
| $\Delta G$ [kcal mol$^{-1}$] | −2.0 | −1.6 | −2.4 | −1.3 | −3.1 | −1.1 | −3.4 | −0.4 |
| Second binding to halogen bond acceptor [D-A-D] | | | | | | | | |
| $\Delta H$ [kcal mol$^{-1}$] | −14.4 | −14.1 | −14.8 | −13.7 | −15.9 | −14.2 | −16.1 | −13.1 |
| $\Delta G$ [kcal mol$^{-1}$] | 1.2 | 1.6 | 0.9 | 2.3 | 0.2 | 1.6 | 0.0 | 3.2 |
| Second binding to halogen bond donor [A-D-A] | | | | | | | | |
| $\Delta H$ [kcal mol$^{-1}$] | | | −12.8 | −13.3 | | | −16.0 | −12.0 |
| $\Delta G$ [kcal mol$^{-1}$] | | | 0.9 | 1.3 | | | −2.1 | 2.2 |
| [a] M06-2X/def2-TZVP with GD3 dispersion correction at 303.15 K. | | | | | | | | |

finite chain. These chains are then interconnected by a single-point halogen bond toward a second molecule of **2**. The latter is only bound twice, analogously to the co-crystal structure of **1** with *anti-m*2I. The intramolecular iodine–iodine distances in *m*4I clearly indicate a mismatch, as one is way longer (5.13 Å) than the other (4.31 Å, Figure 8 B). In addition, the halogen-bond lengths in the two-point motif are also quite different from each other (3.22 vs. 2.96 Å). Although this was also the case with *syn-m*2I, it seems to be more pronounced in this crystal. DFT-calculations suggest that the second two-point binding of **1** to *m*4I is still energetically favored (see Table 1). It thus seemed likely that the reason for these distortions are crystal packing effects. Indeed, when benzene or dichloromethane instead of pentane or diethyl ether were used for co-crystallization, the desired two-point infinite chain motif was obtained. In both cases, solvent molecules partly fill voids created in the crystal structure by the V-shaped backbone of *m*4I. For the co-crystal obtained from DCM (Figure 8 C), the intramolecular iodine–iodine distances are more similar (4.48 and 4.39 Å), just as expected, although not as similar as in the cocrystal of *p*4I and **2**. However, this asymmetry again seems to be caused by crystal packing and the incorporated solvent molecule. In the cocrystal with benzene (Figure 7 D) this difference is much smaller (4.45 and 4.43 Å). One difference between the two crystal structures is that the DCM molecule has short noncovalent contacts towards both the donor and the acceptor while the benzene molecule does not engage in such short contacts.

To complete the systematic screening, the co-crystals of tetramine **2** with *meta*-terphenyls *syn/anti-m*2I and *m*I4 were missing. Unfortunately, no co-crystallization occurred between either *syn-m*2I or *anti-m*2I and this linker despite multiple attempts in various solvents. Only the co-crystal between *m*4I and tetramine **2** was obtained (Figure 9). Its structure is well in line with the previous findings. To bind in a two-point fashion to **2**, the two iodine substituents on one side of *m*4I move further away from each other via a rotating around the C—C single bonds of the backbone. This results in an iodine–iodine distance of 5.28 Å and enables the double two-point recognition with linker **2**. As a consequence, however, it also decreases the distance between the two opposing iodine atoms to 4.34 Å and thus prevents a second two-point recognition. In-
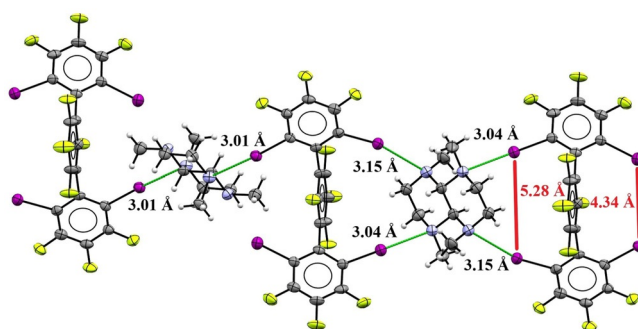


**Figure 9.** Co-crystal structure between linker **2** and halogen bond donor *m*4I (ellipsoids at 50% probability). Halogen bonds are highlighted in green with their corresponding binding distance. Distances between the iodine atoms are highlighted in red. This co-crystal forms an infinite chain topology, alternating between double two-point recognition and single-point recognition.

stead, only a single-point halogen bond is formed to the second moiety of **2**. This is analogous to the co-crystal structure between *p*4I and **1** (Figure 5), just with inverse reasoning on the iodine–iodine distances. In contrast to the latter example, this co-crystal does not form a 2D-network. Instead an infinite chain is observed, with alternating double single- and double two-point halogen bonding.

Finally, our aim was to utilize the deformation of the halogen-bond donor to bind two different substrates within a multipoint-based network: Since the coordination of linker **2** to *m*4I necessitates an elongation of the iodine–iodine distance on the binding side of the halogen-bond donor (Figure 9), our goal was to exploit the concurrent shortening of the iodine–iodine distance on the other side of *m*4I for the coordination of tetramine **1** (which requires such shorter I—I distances, see Figure 8 C).

And indeed, if *m*4I was mixed with both linkers **1** and **2** in a 2:1:1 ratio, co-crystals with both halogen-bond acceptors were obtained (Figure 10). Still, an ideal two-point infinite chain was not observed: while the better fitting acceptor (**1**) was bound by a double two-point recognition motif, the less suitable acceptor (**2**) was bound in a single-point fashion. The intramolecular iodine–iodine distance is 4.40 Å on the side binding tetramine **1** and 4.91 Å on the other side of the halogen-bond
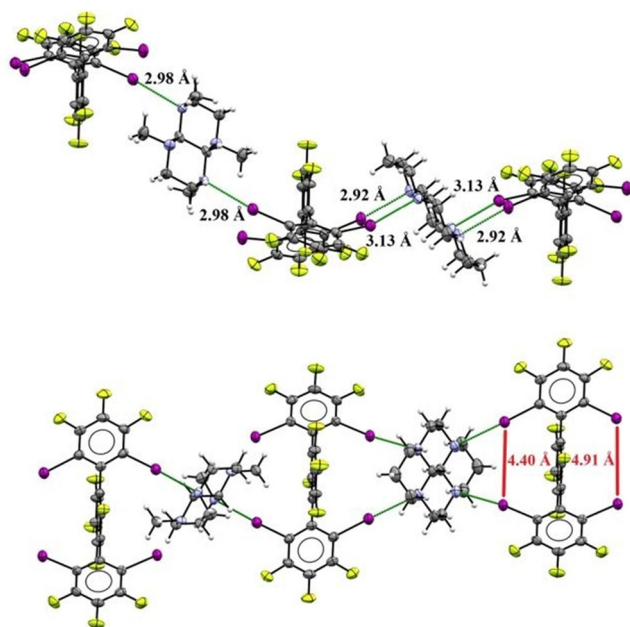
**Figure 10.** Co-crystal structure between tetramines **1** (seen right) and **2** (seen left) as well as halogen-bond donor *m*4I (ellipsoids at 50% probability). Halogen bonds are highlighted in green with their corresponding binding distance. Distances between the iodine atoms are highlighted in red. In this co-crystal, linker **1** is bound by a double two-point interaction, while linker **2** is bound by two single-point interactions.

donor. Unfortunately, the latter is still a bit too close to also bind linker **2** in a two-point fashion in the same crystal.

All experimental studies discussed so far had been accompanied by DFT calculations to help predict and rationalize the findings. This data will be presented in the following discussion. Such insights are particularly valuable since it was difficult to acquire other physical data such as binding constants or thermodynamic properties in solution due to the complex binding modes. With computational methods, however, every binding event could be studied individually.

As computational method of choice, the M06-2X density functional[24] was used as it had been shown to be well-suited for modelling halogen bonding.[25] Grimme's D3 dispersion corrections have been added and have proven to be essential to obtain reasonable results.[26] This is probably due to the somewhat weak strength of halogen bonds between neutral compounds, as for stronger binding adducts involving charged species the contribution of dispersion is usually rather small.[27] Additionally, Cramer and Truhlar's entropy correction[28] was used to account for limitations in the quantum-mechanical harmonic-oscillator approximation for very low-frequency molecular vibrations. This usually leads to an overestimation of the entropy contribution especially for complex systems, as they generate more low frequencies. In our case, it helped to remove outliers with unusually large entropy contributions compared to similar calculations.

In general, the calculations revealed that the binding energies are rather small and do not exceed $-3$ kcal mol$^{-1}$ (Table 1). However, these values are in a reasonable range when compared to reported experimental and theoretical

values for similar systems ranging between single-point and triple-point recognition.[13, 16, 29] While the calculated binding energies in the gas-phase can only provide a very rough estimate of the true binding constants in solution, we can still use this data to explain some of the features of the crystal structures.

The calculated Gibbs free energies of the first binding between *syn-p*2I or *p*4I with **1** or **2** are all relatively similar and in the range of $-1.3$ to $-2.4$ kcal mol$^{-1}$. Tetramine **2** binds slightly weaker in both cases, maybe due to a slightly increased steric hindrance. The second binding event to the halogen bond acceptor is roughly 3 kcal mol$^{-1}$ less favorable compared to the first binding. A larger portion of these loses are due to entropy contributions. The results are similar for the binding of a second acceptor unit to halogen bond donor *p*4I, even though the binding of **2** is now enthalpically favored over **1**, but only marginally and likely within the error of the method.

In the case of *syn-m*2I and *m*4I, the differences in binding to tetramines **1** versus **2** are more pronounced, with linker **1** clearly outcompeting its competitor **2**: while less distinct in the case of *syn-m*2I ($\Delta\Delta G = 2.0$ kcal), **1** binds significantly better to *m*4I than **2** ($\Delta\Delta G = 3.0$ kcal). The reason for this could be the proximity of two iodine substituents. As the binding with linker **2** forces the halogen bond donor to rotate the iodine atoms on the binding site outwards, the opposing iodine atoms get quite close to each other, which may result in repulsion between them. This can also be observed in the corresponding crystal structure (Figure 9). In the calculations involving the complex of *p*4I with **2**, in contrast, the iodine substituents are further away from each other.

While the secondary binding events are also less favored by roughly 3 kcal mol$^{-1}$ for the *meta*-terphenyls, the preference for binding **1** is still existent, especially for *m*4I. Obviously, a direct comparison of these findings with the crystal structures is difficult, but the computed binding strengths at least provide a rough measure of the individual interactions observed within the complex networks. In addition, and maybe more importantly, the distortion of the halogen-bond donors induced by the binders was nicely reproduced in the calculations, and thus the optimized geometries provided an ideal starting point for the search of suitable donor–acceptor pairs.

## Conclusions

In this study, single and double bidentate neutral halogen-bond donors have been used in combination with two different double bidentate acceptors (tetramines) as a tool in crystal engineering. In total, ten out of the twelve possible combinations were indeed obtained as single crystals and were characterized structurally. To the best of our knowledge, a systematic investigation of these kinds of halogen-bonding-based multi-point interactions in the solid state is unprecedented.

The two tetramines employed (**1** and **2**) differed in their respective nitrogen–nitrogen distance for twofold bidentate coordination. The structural analyses clearly identified matching and mismatching pairs with the halogen-bond donors:

In all cases, the single bidentate halogen bond donors (*syn/anti-p*2I and *syn/anti-m*2I) served as reference systems to

study the binding of the tetramines, while the double bidentate variants (*p*4I and *m*4I) were intended as building blocks for extended supramolecular structures, ideally infinite chains based entirely on two-point recognition. Co-crystals with the *anti*-isomers invariably lead to zig–zag chains based on single-point interactions. The *syn*-isomers formed 2:1 complexes between halogen bond donor and tetramine in each case, but with less structural distortions being observed for the pairs *syn*-*p*2I with linker **2** and *syn*-*m*2I with linker **1**. This preference was also found in the structures of the double bidentate halogen-bond donors, where only the combination of *p*4I with **2** or *m*4I with **1** yielded clean infinite chains based on pure two-point recognition. Finally, a co-crystal was also realized involving a 2:1:1 stoichiometry of *m*4I, **1**, and **2**, which feature mixed single- and two-point coordination.

The formation of these binding motifs and topologies is not coincidental. Our study shows how the high directionality of halogen bonding in combination with multipoint binding can be exploited to design such systems. An additional parameter to consider are conformational changes of the halogen-bond donors upon binding, for example, by bending or twisting of the backbone. Depending on the extent of these changes, a second binding site can be altered to either bind differently to a second identical acceptor or to bind to an entirely different type of acceptor. On the other hand, if these changes are minimized by using very well-fitting acceptors, the donor can bind a second acceptor the same way, resulting ultimately in infinite chains which are based on multipoint recognition. We expect these design principles to be of interest for the further development of more sophisticated applications of halogen bonding in supramolecular chemistry and crystal engineering. This is particularly true for systems in which the response to conformational changes can be used as a probe.

## Acknowledgements

## Conflict of interest

The authors declare no conflict of interest.

[1] a) A. C. Legon, *Phys. Chem. Chem. Phys.* **2010**, *12*, 7736–7747; b) G. R. Desiraju, P. S. Ho, L. Kloo, A. C. Legon, R. Marquardt, P. Metrangolo, P. Politzer, G. Resnati, K. Rissanen, *Pure Appl. Chem.* **2013**, *85*, 1711–1713.

[2] a) A. C. Legon, H. E. Warner, *J. Chem. Phys.* **1993**, *98*, 3827–3832; b) R. Weiss, O. Schwab, F. Hampel, *Chem. Eur. J.* **1999**, *5*, 968–974; c) R. Weiss, G. E. Miess, A. Haller, W. Reinhardt, *Angew. Chem. Int. Ed. Engl.* **1986**, *25*, 103–104; *Angew. Chem.* **1986**, *98*, 102–103; d) R. Weiss, M. Rechinger, F. Hampel, *Angew. Chem. Int. Ed. Engl.* **1994**, *33*, 893–895; *Angew. Chem.* **1994**, *106*, 901–903.

[3] a) M. T. Messina, P. Metrangolo, W. Panzeri, E. Ragg, G. Resnati, *Tetrahedron Lett.* **1998**, *39*, 9069–9072; b) P. Metrangolo, G. Resnati, *Chem. Eur. J.* **2001**, *7*, 2511–2519.

[4] P. Metrangolo, G. Resnati, T. Pilati, S. Biella in *Halogen Bonding: Fundamentals and Applications, Vol. 126*, Springer, Berlin, Heidelberg **2008**, pp. 105–136.

[5] Reviews and selected examples: a) R. B. Walsh, C. W. Padgett, P. Metrangolo, G. Resnati, T. W. Hanks, W. T. Pennington, *Cryst. Growth Des.* **2001**, *1*, 165–175; b) K. Rissanen, *CrystEngComm* **2008**, *10*, 1107–1113; c) N. K. Beyeh, F. Pan, K. Rissanen, *Angew. Chem. Int. Ed.* **2015**, *54*, 7303–7307; *Angew. Chem.* **2015**, *127*, 7411–7415; d) G. Cavallo, P. Metrangolo, R. Milani, T. Pilati, A. Priimagi, G. Resnati, G. Terraneo, *Chem. Rev.* **2016**, *116*, 2478–2601; e) C. B. Aakeröy, S. V. Panikkattu, P. D. Chopade, J. Desper, *CrystEngComm* **2013**, *15*, 3125–3136; f) A. Mukherjee, S. Tothadi, G. R. Desiraju, *Acc. Chem. Res.* **2014**, *47*, 2514–2524; g) H. L. Nguyen, P. N. Horton, M. B. Hursthouse, A. C. Legon, D. W. Bruce, *J. Am. Chem. Soc.* **2004**, *126*, 16–17; h) D. W. Bruce, P. Metrangolo, F. Meyer, T. Pilati, C. Präsang, G. Resnati, G. Terraneo, S. G. Wainwright, A. C. Whitwood, *Chem. Eur. J.* **2010**, *16*, 9511–9524; i) H. M. Yamamoto, J. I. Yamaura, R. Kato, *J. Am. Chem. Soc.* **1998**, *120*, 5905–5913; j) M. Fourmigué, P. Batail, *Chem. Rev.* **2004**, *104*, 5379–5418; k) C. B. Aakeröy, C. L. Spartz, *Top. Curr. Chem.* **2014**, *358*, 155–182; l) H. D. Arman, R. L. Gieseking, T. W. Hanks, W. T. Pennington, *Chem. Commun.* **2010**, *46*, 1854–1856; m) H. D. Arman, E. R. Rafferty, C. A. Bayse, W. T. Pennington, *Cryst. Growth Des.* **2012**, *12*, 4315–4323.

[6] a) P. Metrangolo, H. Neukirch, T. Pilati, G. Resnati, *Acc. Chem. Res.* **2005**, *38*, 386–395; b) N. Busschaert, C. Caltagirone, W. Van Rossom, P. A. Gale, *Chem. Rev.* **2015**, *115*, 8038–8155; c) A. Mele, P. Metrangolo, H. Neukirch, T. Pilati, G. Resnati, *J. Am. Chem. Soc.* **2005**, *127*, 14972–14973; d) M. G. Chudzinski, C. A. McClary, M. S. Taylor, *J. Am. Chem. Soc.* **2011**, *133*, 10559; e) C. J. Massena, A. M. S. Riel, G. F. Neuhaus, D. A. Decato, O. B. Berryman, *Chem. Commun.* **2015**, *51*, 1417–1420; f) J. Y. C. Lim, I. Marques, V. Félix, P. D. Beer, *J. Am. Chem. Soc.* **2017**, *139*, 12228–12239.

[7] a) A. Vargas Jentzsch, D. Emery, J. Mareda, P. Metrangolo, G. Resnati, S. Matile, *Angew. Chem. Int. Ed.* **2011**, *50*, 11675–11678; *Angew. Chem.* **2011**, *123*, 11879–11882; b) A. Vargas Jentzsch, A. Hennig, J. Mareda, S. Matile, *Acc. Chem. Res.* **2013**, *46*, 2791–2800; c) A. V. Jentzsch, S. Matile, *Top. Curr. Chem.* **2015**, *358*, 205–239.

[8] a) D. Bulfield, S. M. Huber, *Chem. Eur. J.* **2016**, *22*, 14434–14450; b) S. H. Jungbauer, S. M. Huber, *J. Am. Chem. Soc.* **2015**, *137*, 12110–12120; c) F. Kniep, S. H. Jungbauer, Q. Zhang, S. M. Walter, S. Schindler, I. Schnapperelle, E. Herdtweck, S. M. Huber, *Angew. Chem. Int. Ed.* **2013**, *52*, 7028–7032; *Angew. Chem.* **2013**, *125*, 7166–7170; d) Y. Takeda, D. Hisakuni, C. H. Lin, S. Minakata, *Org. Lett.* **2015**, *17*, 318–321; e) J.-P. Gliese, S. H. Jungbauer, S. M. Huber, *Chem. Commun.* **2017**, *53*, 12052–12055; f) A. Dreger, E. Engelage, B. Mallick, P. D. Beer, S. M. Huber, *Chem. Commun.* **2018**, *54*, 4013–4016; g) W. He, Y. C. Ge, C. H. Tan, *Org. Lett.* **2014**, *16*, 3244–3247; h) A. Bruckmann, M. A. Pena, C. Bolm, *Synlett* **2008**, 900–902; i) S. Kuwano, T. Suzuki, Y. Hosaka, T. Arai, *Chem. Commun.* **2018**, *54*, 3847–3850.

[9] a) S. M. Huber, J. D. Scanlon, E. Jimenez-Izal, J. M. Ugalde, I. Infante, *Phys. Chem. Chem. Phys.* **2013**, *15*, 10350–10357; b) T. Clark, M. Hennemann, J. Murray, P. Politzer, *J. Mol. Model.* **2007**, *13*, 291–296; c) K. E. Riley, P. Hobza, *Phys. Chem. Chem. Phys.* **2013**, *15*, 17742–17751; d) C. W. Wang, D. Danovich, Y. R. Mo, S. Shaik, *J. Chem. Theory Comput.* **2014**, *10*, 3726–3737.

[10] A. Priimagi, G. Cavallo, P. Metrangolo, G. Resnati, *Acc. Chem. Res.* **2013**, *46*, 2686–2695.

[11] a) A. De Santis, A. Forni, R. Liantonio, P. Metrangolo, T. Pilati, G. Resnati, *Chem. Eur. J.* **2003**, *9*, 3974–3983; b) S. V. Lindeman, J. Hecht, J. K. Kochi, *J. Am. Chem. Soc.* **2003**, *125*, 11597–11606.

[12] a) E. A. L. Gillis, M. Demireva, M. G. Sarwar, M. G. Chudzinski, M. S. Taylor, E. R. Williams, T. D. Fridgen, *Phys. Chem. Chem. Phys.* **2013**, *15*, 7638–7647; b) A. Caballero, N. G. White, P. D. Beer, *Angew. Chem. Int. Ed.* **2011**, *50*, 1845–1848; *Angew. Chem.* **2011**, *123*, 1885–1888; c) L. C. Gilday, N. G. White, P. D. Beer, *Dalton Trans.* **2013**, *42*, 15766–15773.

[13] J. Stoesser, G. Rojas, D. Bulfield, P. I. Hidalgo, J. Pasan, C. Ruiz-Perez, C. A. Jimenez, S. M. Huber, *New J. Chem.* **2018**, *42*, 10476–10480.

[14] K. Hervé, O. Cador, S. Golhen, K. Costuas, J.-F. Halet, T. Shirahata, T. Muto, T. Imakubo, A. Miyazaki, L. Ouahab, *Chem. Mater.* **2006**, *18*, 790–797.

[15] a) D. Cao, M. Hong, A. K. Blackburn, Z. C. Liu, J. M. Holcroft, J. F. Stoddart, *Chem. Sci.* **2014**, *5*, 4242–4248; b) S. M. Oburn, N. P. Bowling, E. Bosch, *Cryst. Growth Des.* **2015**, *15*, 1112–1118; c) Y. Takeda, K. Hatanaka, T. Nishida, S. Minakata, *Chem. Eur. J.* **2016**, *22*, 10360–10364; d) L. Maugeri, J. Asencio-Hernández, T. Lébl, D. B. Cordes, A. M. Z. Slawin, M.-A. Delsuc, D. Philp, *Chem. Sci.* **2016**, *7*, 6422–6428; e) L. Maugeri, E. M. G. Jamieson, D. B. Cordes, A. M. Z. Slawin, D. Philp, *Chem. Sci.* **2017**, *8*, 938–945.

[16] S. H. Jungbauer, D. Bulfield, F. Kniep, C. W. Lehmann, E. Herdtweck, S. M. Huber, *J. Am. Chem. Soc.* **2014**, *136*, 16740–16743.

[17] C. B. Aakeröy, A. Rajbanshi, P. Metrangolo, G. Resnati, M. F. Parisi, J. Desper, T. Pilati, *CrystEngComm.* **2012**, *14*, 6366–6368.

[18] O. Dumele, N. Trapp, F. Diederich, *Angew. Chem. Int. Ed.* **2015**, *54*, 12339–12344; *Angew. Chem.* **2015**, *127*, 12516–12521.

[19] A. Vanderkooy, M. S. Taylor, *J. Am. Chem. Soc.* **2015**, *137*, 5080–5086.

[20] a) MacGillivray and co-workers have reported halogen-bonded two-point recognition motifs in the solid phase, but in these cases the halogen-bond acceptor (M. A. Sinnwell, L. R. MacGillivray, *Angew. Chem. Int. Ed.* **2016**, *55*, 3477–3480; *Angew. Chem.* **2016**, *128*, 3538–3541) b) or donor (M. A. Sinnwell, J. N. Blad, L. R. Thomas, L. R. MacGillivray, *IUCrJ* **2018**, *5*, 491–496) acted as a template to form a fitting counterpart by [2+2] photodimerization.

[21] J. Ammer, M. Baidya, S. Kobayashi, H. Mayr, *J. Phys. Org. Chem.* **2010**, *23*, 1029–1035.

[22] R. L. Willer, D. W. Moore, C. K. Lowe-Ma, D. J. Vanderah, *J. Org. Chem.* **1985**, *50*, 2368–2372.

[23] P. Metrangolo, G. Resnati, *IUCrJ* **2014**, *1*, 5–7.

[24] Y. Zhao, D. G. Truhlar, *Theor. Chem. Acc.* **2008**, *120*, 215–241.

[25] a) S. Kozuch, J. M. L. Martin, *J. Chem. Theory Comput.* **2013**, *9*, 1918–1931; b) A. Otero-de-la-Roza, E. R. Johnson, G. A. DiLabio, *J. Chem. Theory Comput.* **2014**, *10*, 5436–5447.

[26] S. Grimme, J. Antony, S. Ehrlich, H. Krieg, *J. Chem. Phys.* **2010**, *132*, 154104.

[27] J. Thirman, E. Engelage, S. M. Huber, M. Head-Gordon, *Phys. Chem. Chem. Phys.* **2018**, *20*, 905–915.

[28] R. F. Ribeiro, A. V. Marenich, C. J. Cramer, D. G. Truhlar, *J. Phys. Chem. B* **2011**, *115*, 14556–14562.

[29] M. G. Sarwar, B. Dragisic, L. J. Salsberg, C. Gouliaras, M. S. Taylor, *J. Am. Chem. Soc.* **2010**, *132*, 1646–1653.